Geometrical Effects in Gyrotron Coaxial Cavities: Application to Mode Selection

J. J. Barroso, P. J. Castro, and R. A. Corrêa

Abstract— **A study of the electrodynamical properties of gyrotron coaxial cavities using a conical inner rod has been conducted and compared with cold-test measurements on TE modes over the frequency range 11–14 GHz. On the basis of a geometrical design criterion for resonance of the normal modes, it has been demonstrated that the mode spectrum associated with a purpose-built test coaxial cavity is significantly less dense than that for the empty cavity without the coaxial insert.**

I. Introduction

Recently, overmoded coaxial cavities have found applications in high-power gyrotrons [1] where a straight cylindrical circular inner rod is used to shift the resonant frequencies of competing modes. We examine here the electrodynamical properties of cylindrical coaxial cavities using a conical inner rod on the basis of a geometrical criterion for resonance of the eigenmodes. The modeling of a coaxial cavity, along with experimental results, demonstrates that some TE modes in the range 11–14 GHz are suppressed as a result of the action of the conical coaxial insert.

The remainder of this paper is organized as follows: Section II outlines the formalism adopted for analyzing gyrotron coaxial cavities, whereas, the effects of the inner conductor geometry upon the selective properties of the cavity are explored in Section III. Calculated and measured results are discussed in Section IV, and, finally, Section V contains the conclusions of our work.

II. Normal Modes in Coaxial Gyrotron Cavities

We shall consider the open coaxial cavity type as depicted in Fig. 1. The inner conductor is a conical rod, whereas, the outer cylinder consists of a weakly irregular waveguide with a uniform cylindrical mid-section joined to two linear tapers. For good conductors, the resonant frequencies are close to the cutoff frequencies $\omega_c = c\chi_{mp}/b$, where c is the speed of light, b is the outer waveguide radius, and χ_{mp} denotes the p-th nontrivial root of the Bessel-Neumann combination

$$J'_m(\chi_{mp})N'_m(\chi_{mp}/C) - J'_m(\chi_{mp}/C)N'_m(\chi_{mp}) = 0. \quad (1)$$

The parameter $C = b/a$ is defined as the ratio of the inside radius of the outer cylinder to the radius of the inner one. For large values of C, the quantity χ_{mp} approaches the root of the equation $J'_m(\chi_{mp}) = 0$, which determines the eigenfrequencies of the hollow cylindrical resonator. The dependence of root χ_{mp} on parameter C is shown in Fig. 2, where one can see the distinctive behavior of the $\chi_{mp}(C)$ curve for the various classes of modes. In particular, for $p = 3$ volume modes, the roots χ_{mp} and, in consequence, the corresponding eigenfrequencies rapidly increase as $C \to 2$.

III. Mode Selection from Geometrical Effects

The effects of the inner conductor geometry upon the cavity selective properties can be explained by considering an equivalent empty resonator so that a given normal mode has the same resonant frequency and diffractive Q-factor in both resonators. In this context, a coaxial resonator turns out to be equivalent to an empty one with a longitudinal profile [2], [3]

$$b_{eq}(z) = b(z) - (b(z) - \bar{C}a(z))\frac{C}{\chi}\frac{d\chi}{dC}\bigg|_{\bar{C}} \quad (2)$$

where $\bar{C}$ denotes the average value of C over the interval $0 \le z \le d_1 + d_2$ (Fig. 1). Hence, if the derivative $d\chi/dC$ is negative (positive) at $C = \bar{C}$ and $\theta_c > 0$ ($\theta_c < 0$), the input section of the equivalent empty resonator is a truncated cone narrowing to the cavity output provided the following relation

$$\frac{\bar{C}|T|}{1-T} > \frac{\tan\theta_i}{\tan|\theta_C|} \quad (3)$$

holds, where $T \equiv (C/\chi)(d\chi/d_C)|_{\bar{C}}$. As a result, modes satisfying (3) do not suffer a total reflection on the left side of the main resonant mid section, and, in consequence, cannot resonate. By means of the ensuing set of curves as displayed in Fig. 3, the resonance condition (3) is now used to examine the selective properties of a 3.2-design C

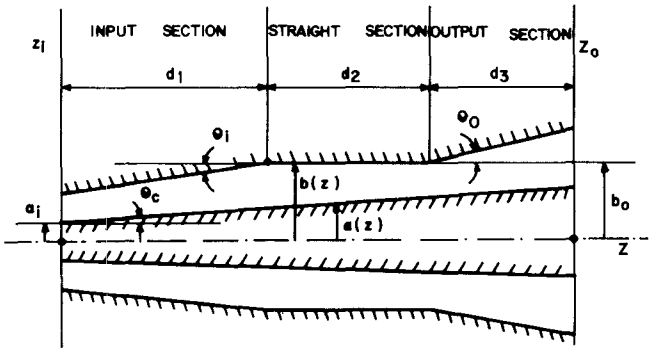

Fig. 1. Schematic diagram of the coaxial resonator along with geometric parameters.

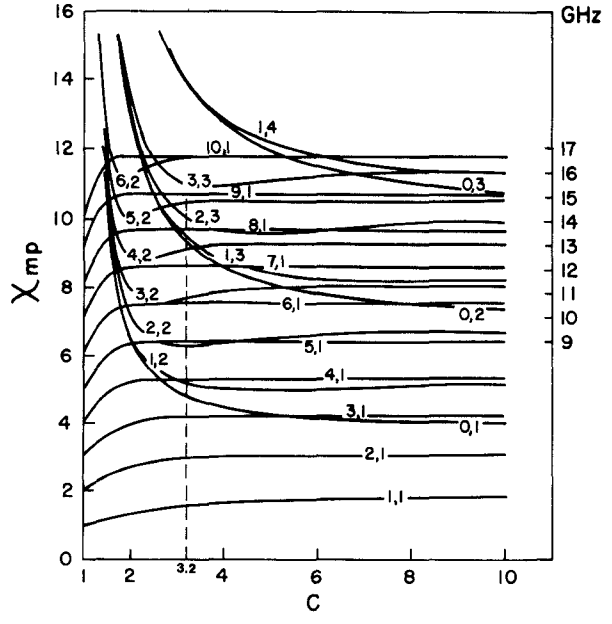

Fig. 2. Dependence of χ_{mp} on parameter C for some TE modes. The right vertical scale gives the cutoff frequency $f_c = c\chi_{mp}/2\pi b_o$ for $b_o = 3.36$ cm.

Manuscript received April 13, 1994; revised October 4, 1994.

The authors are with Laboratório Associado de Plasma, Instituto Nacional de Pesquisas Espaciais, C.P. 515, 12201-970-São José do Campos, SP, Brazil.

IEEE Log Number 9410719.

TABLE I
MEASURED AND CALCULATED VALUES OF RESONANT FREQUENCIES AND Q_T FACTORS FOR FUNDAMENTAL TE MODES

	calculated		measured	
mode TE_{mp}	f [GHz]	Q_T	$(f \pm 20 \times 10^{-1})$ [GHz]	Q_T
3,2	11.1487	1052	11.1408	954
7,1	12.1835	1324	12.1641	1217
4,2	13.1091	1558	13.0917	1381
8,1	13.6984	1655	13.6762	1373
2,3	13.7073	1905	13.7082	1715

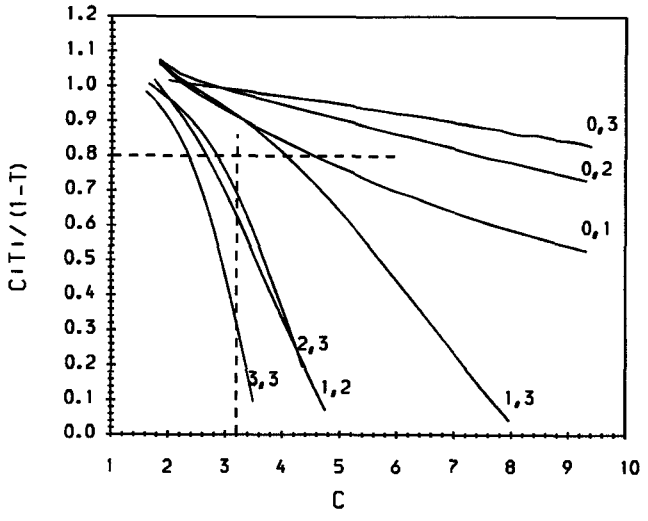

Fig. 3. $C|T|/(1-T)$ as function of parameter C where $T \equiv (C/\chi)(d\chi/dC)$. Only modes from Fig. 2 with negative $d\chi/dC$ slope in the C-interval 3.2–4.0 have been included in this plot.

cavity. In that cavity, the geometric parameters $\theta_i = 0.8°$, $\theta_o = 3.0$, $d_1 = 10.50$ cm, $d_2 = d_3 = 15.75$ cm, and $b_0 = 3.36$ cm define the outer waveguide with $a_i = 0.68$ cm and $\theta_c = 1.0°$ determining the conical inner rod. Thus, we conclude from Fig. 3 that the circularly symmetric modes (TE_{01}, TE_{02}, and TE_{03}) in addition to the volume mode $TE_{1,3}$ are all suppressed, as (3) does apply to such modes. Note in Fig. 4(a), however, that the mid-section of the equivalent empty resonator for the $TE_{2,3}$ mode is a truncated cone that narrows to the output section, as the corresponding $\chi(C)$ curve (Fig. 2) has a negative slope around $C = 3.2$. This yields an exceedingly high diffractive Q_D factor ($>1.0\times10^6$) for the fundamental $TE_{2,3,1}$ mode, with calculations indicating intolerably high Q_D factors ($>1.0\times10^5$) for higher axial order modes $TE_{2,3,q}$ with $q \geq 2$. To circumvent such a drawback posed by the fully-conical inner rod, we resort to considering a cylindrical coaxial insert with a constant radius along the output and mid-sections, while keeping a conical shape in the input section. On adopting this geometry for the inner rod, where $\theta_c = 1.0°$, $a_i = 0.68$ cm, and $a(z \geq d_1) = 0.87$ cm such that $\bar{C} = 3.9$, we can now see in Fig. 4(b) that the mid-section for the equivalent empty resonator is a uniform circular cylinder with radius $b_o = 3.63$ cm. This gives for the $TE_{2,3,1}$ mode a diffractive Q-factor $Q_D = 2140$ nearly equal to that in the empty cavity. Moreover, as displayed in Fig. 3, the circularly symmetric modes as well as the volume $TE_{1,3}$ mode remain still suppressed in this new cavity configuration with $\bar{C} = 3.9$.

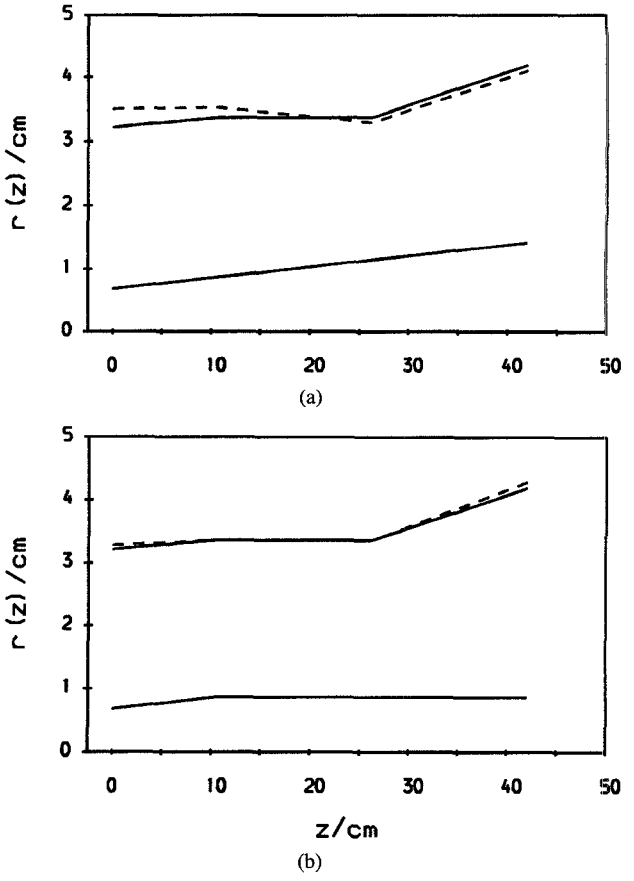

Fig. 4. Longitudinal profiles for the coaxial (solid line) and equivalent empty resonators (dashed line) for $TE_{2,3}$ mode with (a) full conical and (b) partially conical inner rods.

IV. EXPERIMENTAL INVESTIGATION

The selective properties of the 3.9-design C coaxial cavity were experimentally investigated using an HP8510B vector network analyzer, which includes an integrated synthesized source. TE modes were excited by means of a standard WR-90 rectangular waveguide feeding a 7.0-mm-diameter coupling hole drilled through the center of the resonator mid-section. To collect the power reradiated by the resonator, we used a horn gain antenna that was properly positioned to maximize the signal intensity and to avoid any possible distortions in the resonance curve. The Q-factor measured is the total $Q_T = Q_D Q_\Omega/(Q_D + Q_\Omega)$ as determined directly from frequency readings at the half-power points on the detected spectrum. The cavity external structure is a single electroformed copper piece, for which an electrical resistivity of $\sigma_b = 3.8 \times 10^7$ S/m has been assumed, whereas, the inner rod is made from aluminum ($\sigma_a = 2.5\times10^7$ S/m).

To verify the findings anticipated by theory, resonant frequency and Q_T-factor measurements were performed in the frequency range 11–14 GHz. Experimental results are presented in Table I, which confirms the $TE_{1,3}$— and $TE_{0,2}$—mode suppression. In fact, if the $TE_{0,2}$ and $TE_{1,3}$ modes were present, their corresponding eigenfrequencies would be around 12.1 GHz and 12.5 GHz according to Fig. 2. However, after scanning the 11–14-GHz frequency range, no such modes were detected. In this way, the $TE_{7,1}$ mode becomes well isolated from its closest competitors by a frequency spacing of 1.0 GHz.

Finally, it should be noted in Table I that measured Q_T values are typically below the calculated ones by a 10% factor, except for the surface $TE_{7,1}$ and $TE_{8,1}$ modes. This arises from the fact that the

corresponding angular wavelength ($\pi b_o/m$) of these modes is on the order of the coupling hole size, which thus provides an extra energy loss mechanism for such surfaces modes.

V. Conclusion

A study of open coaxial resonators was addressed giving emphasis to the influence of the inner conductor geometry on the cavity selective properties. Making use of a geometrical design criterion for resonance of TE eigenmodes, a cavity was constructed and cold-tested in the frequency range 11–14 GHz. In agreement with theory, it was then demonstrated that some modes were effectively suppressed when introducing a coaxial insert of suitable shape into the empty cavity.

References

[1] M. E. Read, G. S. Nusinovich, O. Dumbrajs, H. Q. Dinh, D. Opie, G. Bird, K. Kreischer, and M. Blank, "Design of a 3 MW, 140 GHz gyrotron based on a $TE_{21,13}$ coaxial cavity," in *Proc. 18th Int. Conf. Infrared Millimeter Waves*, Colchester, England, vol. SPIE 2104, 1993, p. 521.

[2] J. J. Barroso and R. A. Correa, "Coaxial resonator for a megawatt, 280 GHz gyrotron," *Int. J. Infrared Millimeter Waves*, vol. 12, no. 7, p. 717, 1991.

[3] S. N. Vlasov, L. I. Zagrydskaya, and I. M. Orlova, "Open coaxial resonators for gyrotrons," *Radio Eng. Electron. Phys.*, vol. 21, no. 5, p. 96, 1976.

[4] P. J. Castro, J. J. Barroso, and R. A. Correa, "Cold tests of a 10 GHz gyrotron cavity," *Int. J. Infrared Millimeter Waves*, vol. 13, no. 1, p. 91, 1992.

Condition for Distortionless Transmission Line with a Nonuniform Characteristic Impedance

Jonas Lundstedt

***Abstract*—The well-known condition for distortionless signal propagation on a dissipative transmission line with constant impedance is generalized to the case of nonuniform impedance. The result is based on a time-domain wave-splitting formulation of the Telegraphist's equations. It is shown that an appropriate choice of the resistance and the conductance can eliminate the distortion caused by the varying characteristic impedance. A nonuniform transmission line that satisfies the given condition is distortionless in both directions, but reflectionless for signals propagating in one direction only.**

I. Introduction

O. Heaviside derived the well-known condition for distortionless lines that states that the resistance and the conductance can be matched to each other so that the distortion vanishes on transmission lines with constant impedance. Matching of two lines with different impedance with a transmission line taper is usually done with a lossless line in order to preserve the energy of the signal at the cost of a limited bandwidth. We present a condition for distortionless *nonuniform* transmission lines. It is shown that it is possible to match the resistance and conductance to the slope of the impedance so that the signal propagates undistorted with no reflections in one direction and undistorted but with reflections in the other direction. One consequence is that it is possible to design a perfect impedance match if energy loss is acceptable. The idea to this distortionless condition has evolved from the work in [1].

Manuscript received February 7, 1994; revised October 3, 1994.

The author is with the Royal Institute of Technology, Department of Electromagnetic Theory, S-100 44 Stockholm, Sweden.

IEEE Log Number 9410720.

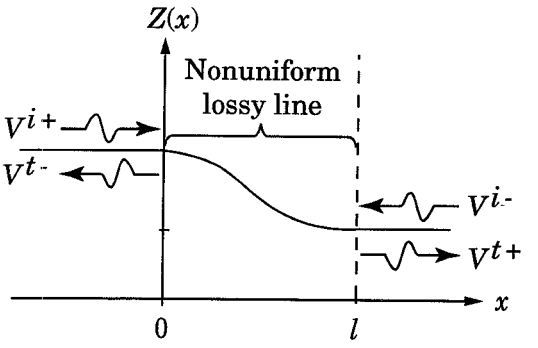

Fig. 1. The nonuniform and lossy transmission line between $x = 0$ and $x = l$ is imbedded between two uniform and lossless transmission lines.

II. The Telegraphist's Equations and the Wave-Splitting

Consider a nonuniform LCRG transmission line with length l, which is imbedded between two uniform and lossless LC transmission lines. Incident signals from the left and right side of the uniform line are denoted V^{i+} and V^{i-}, respectively. The signal generators are assumed to be impedance matched. At $x = 0$, a left-moving wave, V^{t-}, is due to transmission of the incident signal V^{i-} and reflection of V^{i+}. The corresponding right-moving wave at $x = l$ is denoted V^{t+}.

For a TEM transmission line, the voltage V and the current I satisfy the Telegraphist's equations

$$\frac{\partial}{\partial x}\begin{bmatrix} V(x,t) \\ I(x,t) \end{bmatrix} = \begin{bmatrix} 0 & -R(x) - L(x)\dfrac{\partial}{\partial t} \\ -G(x) - C(x)\dfrac{\partial}{\partial t} & 0 \end{bmatrix} \cdot \begin{bmatrix} V(x,t) \\ I(x,t) \end{bmatrix} \tag{1}$$

where $L(x), C(x), R(x)$, and $G(x)$ are respectively, the inductance, capacitance, series resistance, and shunt conductance of the line. The local characteristic impedance, $Z(x)$, and local wavefront speed, $c(x)$, are defined as

$$Z(x) = \frac{1}{Y(x)} = \sqrt{\frac{L(x)}{C(x)}}, \quad c(x) = \frac{1}{\sqrt{L(x)C(x)}}. \tag{2}$$

On a lossless and homogeneous transmission line, the solution to (1) can be decomposed into two parts, V^+ and V^-, which represent right-moving and left-moving waves, respectively

$$\begin{cases} V^+(x,t) = V^+(t - x/c) = ZI^+(t - x/c) \\ V^-(x,t) = V^-(t + x/c) = -ZI^-(t + x/c) \end{cases} \tag{3}$$

where I^+ and I^- are the currents that correspond to V^+ and V^-, respectively. The relation between V^+, V^- and the total voltage and